E12-11-003B

Study of J/ψ Photoproduction off Deuteron

(Run Group B Proposal)

M.D. Baker
MDB Physics and Detector Simulations LLC, Miller Place, NY 11764
A.J. Freese
Argonne National Laboratory, Lemont, IL 60439, USA
L. Guo
Florida International University, Miami, FL 33199, USA
Ch. Hyde
Old Dominion University, Norfolk, VA 23529, USA
Y. Ilieva*(co-spokesperson)
University of South Carolina, Columbia, SC 29205, USA

B. McKinnon(co-spokesperson)
University of Glasgow, Glasgow G12 8QQ, UK

P. Nadel-Turonski(co-spokesperson)
Stony Brook University, Stony Brook, NY 11794, USA

M. Sargsian
Florida International University, Miami, FL 33199, USA

V. Kubarovsky(co-spokesperson), S. Stepanyan(co-spokesperson)
Thomas Jefferson National Accelerator Facility, Newport News, VA 23606, USA

N. Zachariou
Edinburgh University, Edinburgh EH9 3JZ, UK

Z.W. Zhao(co-spokesperson)
Duke University, Durham, NC 27708, USA

June 4, 2018

*ilieva@sc.edu

Abstract

Exclusive, near-threshold quasi-real photoproduction of J/ψ off the deuteron provides attractive opportunities to study interesting physics. Besides studying the gluonic structure of bound nucleons and the deuteron (in coherent production), studying the final-state interactions allows a direct access to the elementary J/ψN cross section. There is one measurement of the near-threshold quasi-elastic J/ψ production off the deuteron, however data on final-state interactions or of the coherent cross section do not exist. With its high luminosity and large acceptance, the CLAS12 detector is well suited to measure near-threshold photoproduction of J/ψ off the deuteron.

This is a proposal to measure the differential cross section of the incoherent and the coherent production of J/ψ meson off the deuteron. The reactions $\gamma d \to J/\psi pn$ and $\gamma d \to J/\psi d$ will be measured in untagged quasi-real photoproduction, where all the final state particles (the nucleon(s) or deuteron, and the lepton pair from the J/ψ decay) are detected and the photon is reconstructed via 4-momentum conservation. The incoherent measurement will provide data on the gluon form factors of bound nucleons and on the J/ψN interaction. The coherent measurement will be the first measurement, albeit with low statistics, of the gluonic structure of the deuteron. The same reactions will also be accessed with the Forward Tagger (FT), where the small-Q^2 photon kinematics is measured by the FT and all but one final-state particles are detected in the CLAS12.

We will be able to measure J/ψ production off the quasi-free neutron by measuring a high-energy (p $>$ 1 GeV/c) neutron in the CLAS forward calorimeters in the fully exclusive untagged real photoproduction and will be in position to search for isospin partners of the LHCb pentaquarks $P_c^0(4380)$ and $P_c^0(4450)$.

This is a run-group proposal to join Run Group B (RG B). RG B provides a window of opportunity for a first measurement at JLab of these processes. The measurement considered here does not require any additional detection system than already planned for RG B. We will need an additional trigger for charged particles in opposite sectors that will add 20% to the trigger rate. This trigger was tested and used by Run Group A in their 2018 run. The proposal is an extension of the E12-12-001 experiment.

Contents

1 Introduction

With the 12-GeV Jefferson-Lab upgrade providing beam energies above the threshold for photoproduction of J/ψ off the nucleon, interest in near-threshold J/ψ photoproduction has risen in both the experimental and the theoretical communities. The near-threshold exclusive photoproduction off the proton will be studied in several approved experiments in Halls A, B, and C. There are some physics aspects of the J/ψ production dynamics that these studies will not be able to address and that can be answered by using deuteron as a target. This program will provide the very first measurement of exclusive J/ψ photoproduction off deuteron from threshold up to 11 GeV and at $Q^2 = 0 - 0.02$ (GeV/c)^2. The measurement will allow to access the complementary but yet unexplored J/ψ photoproduction off the neutron channel and possibly to measure the coherent process on the nucleus. There are several exciting physics problems that the proposed program is uniquely positioned to address: by accessing directly the $J/\psi N$ elastic scattering in final-state interactions, we will be able to assess the largely unknown low-energy total $J/\psi N$ cross section, by measuring the quasi-free (QF) J/ψ photoproduction off the neutron, we will provide evidence for (or against) a pentaquark decaying into $J/\psi n$, and access the gluonic structure of the deuteron by measuring the coherent process at large momentum transfer. At this time there are no other letters of intent or proposals at JLab involving exclusive J/ψ photoproduction off deuteron. E12-07-106, conditionally approved in Hall C, will measure the A-dependence of the quasi-free J/ψ photoproduction via inclusive J/ψ measurement in an untagged-photon beam experiment on several nuclear targets, including deuteron and proton.

The advantage of the studies presented here originates from the exclusivity of the measurement, which would allow for more precise quantification of the contribution of final-state interactions (FSI) to the incoherent process and for exact treatment of the Fermi momentum of the target nucleon. Also, we will provide a direct measurement of the elementary production off the bound neutron. This proposal is also a precursor for future CLAS12 experiments of J/ψ photoproduction off heavier nuclear targets.

The interest in near-threshold photoproduction of J/ψ off the nucleon stems from the kinematic characteristic of this process. The photon-beam threshold energy is 8.20 GeV, which leads to a small coherence length of the $c\bar{c}$ fluctuation, $l_c \cong 2E_\gamma^{lab}/4m_c^2 = 0.36$ fm [1]. The large mass of the charmed quark and the large minimum momentum transfer $|t_{min}| = 2.2$ (GeV/c)^2 at threshold energy imply that the reaction occurs with a small transverse-size probe and at a small impact parameter. In coherent production off the deuteron, the coherence length is even smaller and $|t_{min}|$ at threshold is larger. Thus, the expectation is that close to threshold the production cross section is sensitive to short-distance correlations in the wave function of the target and to multi-gluon exchange mechanisms [1, 2]. Moreover, FSI in incoherent J/ψ photoproduction off the deuteron provide access to the elementary $J/\psi N$ scattering cross section.

2 Physics Motivation

The 11-GeV electron beam available in Hall B allows to study near-threshold photoproduction of J/ψ in exclusive scattering off deuteron. There are three main physics topics of interest:

- Assessment in a more direct way (than in J/ψ photoproduction off the free proton) of the magnitude of the elementary $J/\psi N$ total cross section by means of final-state interactions in the incoherent photoproduction.
- Assessment of the gluonic form-factor of the deuteron by means of coherent photoproduction $\gamma d \to J/\psi d$.
- Study of J/ψ photoproduction off the neutron by means of quasi-free photoproduction off the bound neutron $\gamma d \to J/\psi n p_s$, where p_s denotes a spectator proton.

As the above studies would need input for the elementary $\gamma p \to J/\psi p$ production, the measurement of differential cross sections in photoproduction off deuteron is well timed as several approved experiments will measure the $\gamma p \to J/\psi p$ reaction prior to or concurrent with the deuteron measurement presented here. Moreover, we will be able to estimate the elementary cross sections for production off both bound proton and neutron.

2.1 Final-State Interactions in Incoherent J/ψ Photoproduction off Deuteron

The study of $J/\psi N$ final-state interactions, with the aim to assess the total low-energy $J/\psi N$ cross section, $\sigma_{J/\psi N}$, is one of the major drivers of the program laid out here. The $J/\psi N$ cross section is an important element in the study of the J/ψ interaction with nucleons and nuclear matter as various theoretical models make predictions for $\sigma_{J/\psi N}$ and these can be directly compared to experimental estimates.

In a simple picture, the near-threshold incoherent reaction $\gamma d \to J/\psi pn$ can be considered to proceed via the following mechanisms (see Fig. 1): (a) quasi-free production off the proton or the neutron, (b) two-step mechanism in which J/ψ is produced in a first step in the quasi-free mechanism off one of the nucleons, followed by a nucleon-nucleon rescattering, NN FSI, and (c) two-step mechanism in which J/ψ is produced in a first step in the quasi-free mechanism off one of the nucleons and than rescatters off the other nucleon, $J/\psi N$ FSI.

The $J/\psi N$ FSI is of particular interest since it provides the most direct experimental access to the $J/\psi N$ total cross section, which is otherwise difficult to measure and is not well understood at low energies [3]. The J/ψ interaction with nuclear matter has been extensively studied at high energies since the experimentally-observed suppression of J/ψ yield in heavy-ion collisions is predicted to be an unambiguous signature of the phase transition from cold nuclear matter to quark-gluon plasma [11]. In order to support the correct interpretation of this J/ψ suppression, high-energy J/ψ production in proton-nucleus collisions has been also

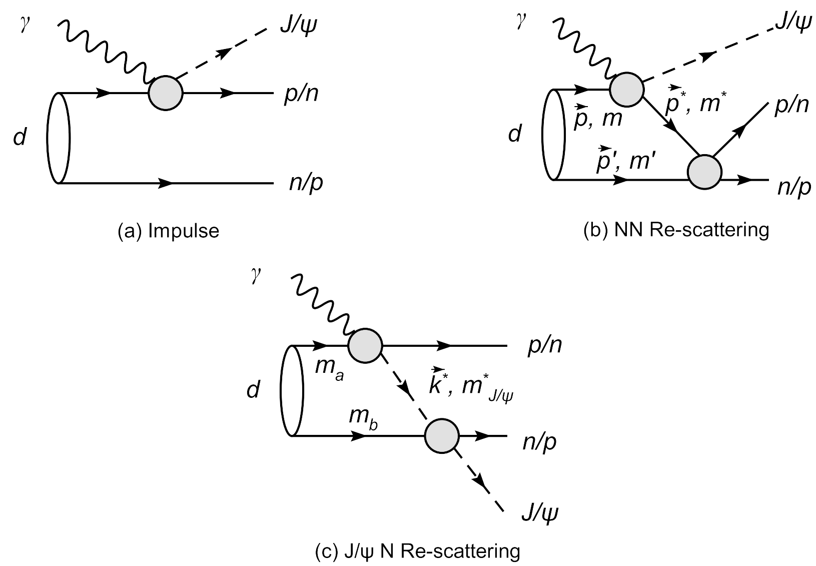

Figure 1: Top Left: A diagram representing the quasi-free mechanism contributing to the incoherent photoproduction of J/ψ off the deuteron. Top Right: A diagram representing the NN final-state interaction. Bottom: A diagram representing the $J/\psi N$ FSI. In an exclusive measurement, a relatively clean QF sample of events can be obtained by selecting events with a low-momentum nucleon (such as below 200 MeV/c). An event sample dominated by FSI can be obtained by selecting events with two high-momentum nucleons. The figure is from Ref. [13], which describes a theoretical model of the incoherent photoproduction of J/ψ off the deuteron that includes quasi-free production and single re-scattering mechanisms.

extensively measured, with the goal to quantify the benchmark "normal nuclear absorption" with respect to which new phenomena can be clearly identified [10]. Due to lack of data, however, the low-energy $J/\psi N$ total cross section is largely unknown. Applying vector-meson dominance to inclusive J/ψ photoproduction data on Be at photon energies $80 - 230$ GeV suggests a total cross section of around 1 mb [4], while the application of an optical model for the rescattering of the J/ψ off the spectator nucleons to inclusive data on Be and Ta at photon energies of 20 GeV indicates a higher value of 3.5 mb [5]. Extrapolations of these values to lower photon energies, such as close to the J/ψ production threshold off a nucleon, are very uncertain.

Concerning theoretical calculations, while two-gluon exchange models predict a monotonically increasing cross section that approaches an asymptotic value at large energies [6], other models that account for non-perturbative effects suggest a rather large value of 17 mb at low energies [7]. The interest in the low-energy $J/\psi N$ cross section stems from the possibility to study the QCD van der Waals potential and possible J/ψ-nuclear bound states. Some analyses suggest that the force between a J/ψ and a nucleon is purely gluonic in nature, and therefore is the analog in QCD of the van der Waals force in electrodynamics, since the hadrons are color neutral objects, and predict that J/ψ-nuclear bound states may exist [8, 9]. The analysis of [9] estimates the low-energy $J/\psi N$ total cross section to be about 7 mb, whereas the analysis of [12] yields a much smaller estimate. It is important to note that the strength of the gluonic van der Waals force between the J/ψ and N is controlled by the chromoelectric polarizability of the vector meson. The differences between the estimates of the $J/\psi N$ cross section in [7], [9], and [12], which are all first-principle theoretical calculations, are to a large extent due to different values of the chromoelectric polarizability calculated in each of these models. Thus, an experimental estimate of the $J/\psi N$ cross section will test the different predictions for the QCD van der Waals interaction. Ideally, one would confront the models with a value of the $J/\psi N$ scattering length extracted from $J/\psi N$ elastic cross-section data. Since J/ψ beams or targets do not exist, the next best option is J/ψ production with final-state interactions.

The 12-GeV upgrade of Jefferson Lab has triggered several theoretical investigations of the feasibility to constrain the value of the total $J/\psi N$ cross section with measurements of incoherent electro- and photo-production of J/ψ off the deuteron [3, 13, 14]. The advantage of the deuteron is that it can be described theoretically with high accuracy and calculations are easier to perform than for heavier nuclei.

The near-threshold incoherent process at $|t| \geq 1$ (GeV/c)^2 has been analyzed in the eikonal approximation in [3]. The analysis considers not only the QF and the single-rescattering mechanisms shown in Fig. 1, but also double-rescattering diagrams. The sensitivity of the reaction to the value of the $J/\psi N$ cross section is demonstrated in the angular dependence of the ratio R on the neutron angle relative to the 3-momentum transfer to the pn system, where R is

$$R = \frac{\sigma(p_n = 600\ \mathrm{MeV/c})}{\sigma(p_n = 200\ \mathrm{MeV/c})}. \tag{1}$$

In this equation, p_n denotes the lab-system momentum of the neutron off which J/ψ rescatters, whereas σ denotes the five-fold differential cross section $\frac{d^5\sigma}{dp_{J/\psi}d\Omega_{J/\psi}d\Omega_p}$ of the reaction $\gamma d \to J/\psi pn$, where $p_{J/\psi}$ is the magnitude of the vector-meson lab-system (LS) 3-momentum, $\Omega_{J/\psi}$ is the vector-meson LS solid angle, and Ω_p is the final-state proton LS solid angle. This angular dependence for several values of $\sigma_{J/\psi N}$ is shown in Fig. 2. One observes large sensitivity at

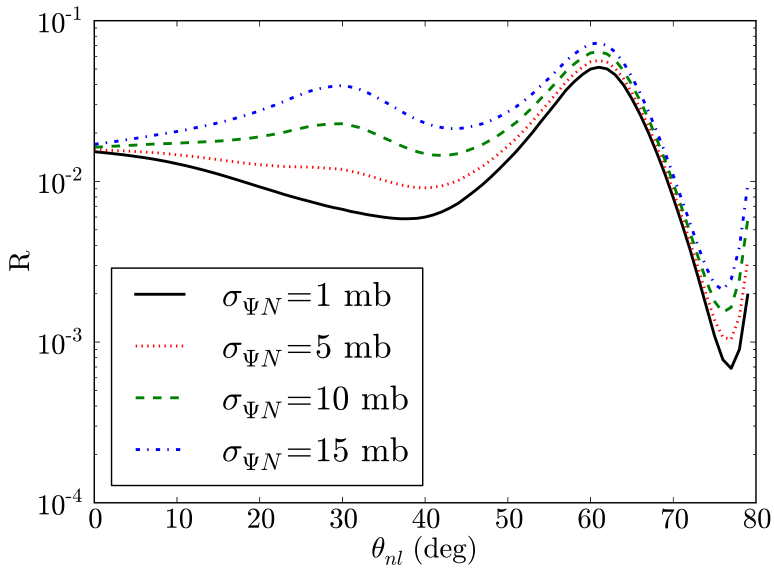

Figure 2: Predictions by the model of [3] for the ratio of Eq. 1 as a function of the neutron angle, θ_{nl}, relative to the 3-momentum transfer to the pn system. The various curves are obtained with different values of $\sigma_{J/\psi N}$. The quasi-free cross section has been calculated using a two-gluon parametrization. One observes large sensitivity at neutron angles around 30°.

neutron angles θ_{nl} about 30°, which correspond to neutron LS angles between 10° and 60° for the photon beam energies available in the proposed experiment. Angles $\theta_{nl} < 30°$ correspond to neutron LS angles between 0° and 50°, whereas $\theta_{nl} > 30°$ correspond to neutron LS angles above 20°. The large angular acceptance of CLAS12 will not only allow us to evaluate the cross-section ratio at neutron lab system angles where the maximum of the $J/\psi N$ rescattering is expected, but also over all the angles covered by the $J/\psi N$ rescattering peak. Moreover, we will be able to assess cross-section ratios not only for $J/\psi n$, but also for $J/\psi p$ FSI.

The near-threshold incoherent process has also been analyzed in the coupled-channel model of [13]. The study considers $J/\psi n$ rescattering and studies the dependence of the cross section of the incoherent process on the $J/\psi N$ potential. Calculations with potentials of various strengths obtained from effective theory approach and lattice QCD have been performed. The study finds that the cross section for forward-scattered protons is more sensitive to the strength of the potential than the cross section for backward scattered protons and identifies kinematics where the $J/\psi N$ FSI dominates the QF and the NN FSI. The most advantageous kinematics is at forward proton scattering angles and energy of the J/ψ in the center-of-mass of the $J/\psi N$ system below $\approx$200 MeV. One should mention that the cross-section predictions of this theoretical analysis do not account for the experimental possibility to reduce the QF contribution by eliminating low-momentum nucleon events. The latter will help to improve the sensitivity of the cross section to the $J/\psi N$ interaction at larger proton angles. Nonetheless, the opportunity to measure the incoherent process with various event topologies will provide access to small nucleon scattering angles. The only limitation will arise from statistics, as nucleons scattered at small angles in the first step of the $J/\psi N$ FSI absorb large momentum transfer and the cross section at these angles is suppressed due to the nucleon form factor. Thus, the possibility to increase the sensitivity to the physics of interest for larger nucleon scattering angles is an important aspect of the exclusive measurement proposed here.

With CLAS12 and photon-beam energies from threshold up to 11 GeV, the J/ψ beam produced in the first step of this FSI has momentum in the range from 5 GeV/c to 10 GeV/c, which provides access to total center-of-mass energies of the $J/\psi N$ system from 4.6 GeV to 5.7 GeV. While we will be able to extract the differential cross section for FSI as a function of t or of the scattered-nucleon angle with respect to the direction of the 3-momentum transfer to the pn system, the extraction of the $J/\psi N$ cross section from these data will be model dependent. The value of the $J/\psi N$ cross section will be obtained by comparing the experimental cross section to model predictions of the same quantity based on different values of the $J/\psi N$ cross section. The $J/\psi N$ cross section that yields the closest match between the prediction and the data will be reported as the extracted cross section. The uncertainties of the model prediction due to the high-momentum tail of the deuteron wave function or the uncertainty in the contribution of np final-state interactions to the predicted $\gamma d \to J/\psi pn$ cross section will contribute to the model-dependent uncertainty of the extracted $J/\psi N$ cross section.

The measurement of the incoherent process over a broad range of scattering angles and momenta of the outgoing nucleons may also provide opportunities to select kinematics where the process is sensitive to scattering off small-size configurations in the deuteron, such as short-range correlations.

2.2 Quasi-Free J/ψ Photoproduction off the Bound Neutron

Here we propose to study elastic production of J/ψ off bound nucleons in the deuteron in quasi-free production regime with the production off the neutron being the central point. Since we will get the production off the bound proton in the data, we refer to both processes as "photoproduction off the bound nucleon" in the discussion below.

The isospin invariance of J/ψ photoproduction is guaranteed by the dominance of gluon exchange in the t-channel. Therefore, there is no reason to expect any difference in the behavior, or the value, of the cross section for J/ψ production off the neutron and off the proton. Nevertheless, this will be not only the first exclusive measurement of J/ψ production off the bound neutron, but also off the bound proton, and as such, will allow to test the bound and free proton gluonic form-factors.

There are three approved experiments in Halls A [16], B [17, 18], and C [19] for studying J/ψ photo- and electroproduction off the proton using a hydrogen target. While there are no J/ψ PAC-approved proposals for Hall D, the GlueX experiment has already presented a J/ψ yield from the first engineering run, and will produce more results on J/ψ photoproduction in the near-threshold region. These measurements will study gluonic form-factors of the proton by measuring the t-dependence of the cross section, and will test the models for J/ψ production mechanism near threshold by measuring the total cross section as a function of the total center-of-mass energy.

After the discovery by LHCb of the hidden-charm pentaquarks $P_c^+(4380)$ and $P_c^+(4450)$ [20], a new objective has been added to the J/ψ photoproduction studies: the production and study of these states as s-channel resonances in photon-proton scattering with subsequent decay $P_c \to J/\psi p$. There are several models on the market that attempt to describe the internal structure of the pentaquarks with hidden charm.

- The P_c states are interpreted as composites of a heavy compact quarkonium state (J/ψ, ψ', or χ $c\bar{c}$ bound states) and light nucleon quarks [21–23]. The dominant decay modes of such pentaquarks are to charmonium states with hidden charm and ordinary baryons. Decays of these hadro-charmonium pentaquarks into states with open charm are strongly suppressed.

- The P_c states are hadronic molecules [25–28]. These molecules consist of a charmed baryon and a charmed meson that are weekly coupled to each other. The distance between the open charm-meson and the baryon is relatively large, which strongly suppresses decays to final states with hidden-charm $c\bar{c}$ mesons. Such pentaquarks will decay predominantly to the charmed baryon and charmed meson.

- Pentaquarks are made of tightly correlated di-quarks or colored baryon-like and meson-like constituents [29–32].

Either of the scenarios listed above predicts a number of new pentaquark states. For example, a hadro-charmonium LHCb pentaquark is a member of an SU(3) flavor octet. It means that the neutral partners of the LHCb pentaquarks exist with almost the same mass and decay probability to $J/\psi + n$ [24]. The situation with a molecular type pentaquark is less clear. The SU(3) partners of such a pentaquark can fail to form bound states. Whether the molecular pentaquarks have isotopic partners remains an open question [23]. Clearly, the experimental search for the resonances decaying into $J/\psi + n$ will clarify the nature of the LHCb pentaquarks and possibly resolve between the models of the discovered hidden-charm pentaquarks.

This measurement, as well as other JLab experiments, will also address the more basic question whether the LHCb pentaquark does exist. If the pentaquark is genuine, then our experiments will find it in the $J/\psi+p$ and $J/\psi+n$ decay modes. What is important specifically for the $J/\psi + n$ production, is that isospin invariance tells us that there are at least two pentaquarks, a positively charged one and an electrically-neutral one. Any "signal" seen in $J/\psi + p$ and not seen in $J/\psi + n$ would remain questionable, so the neutral measurement is vitally important. More so, since production off the deuteron allows to simultaneously measure the $J/\psi + p$ and $J/\psi + n$ final states under the same experimental conditions. The measurement of the $J/\psi+n$ decay mode is valuable also in case "no signal" is seen in $J/\psi+p$, which could be due to a suppressed excitation on the proton, as a strong excitation off the neutron may be the means to confirm the LHCb pentaquark in JLab experiments. There is a similar situation with a suppressed excitation on the proton and a strong excitation on the neutron for N*(1685). The LHCb results may be questionable if JLab experiments do not confirm the pentaquark in photoproduction off the proton and off the neutron. Thus, the importance of testing both final states, $J/\psi + n$ and $J/\psi + p$, is clear.

In the vector-meson dominance (VMD) picture the elastic photoproduction of a vector meson can be related to the vector-meson nucleon scattering, see, *e.g.*, [33]:

$$\frac{d\sigma_{\gamma N\to VN}}{dt} = \mathcal{K}\frac{3\Gamma(V\to e^+e^-)}{\alpha m_V}\frac{d\sigma_{VN\to VN}}{dt}, \tag{2}$$

where $\mathcal{K}$ is a kinematic factor, Γ is the partial decay width of the vector meson to e^+e^-, α and m_V are the fine structure constant and the meson mass, respectively. The physical picture of this process is shown in Fig. 3 [1]. The photon fluctuates into a $\bar{q}q$ pair in some l_C distance before the interaction (coherence length), then the $\bar{q}q$ pair of size $r_\perp$ scatters off the nucleon with impact parameter b, and forms a vector meson at some distance l_F after the scattering (formation length). In the near-threshold J/ψ photoproduction these parameters are much smaller than the nucleon size:

$$l_C \;=\; \frac{2E_\gamma}{4m_c^2} \approx 0.4\ fm,$$

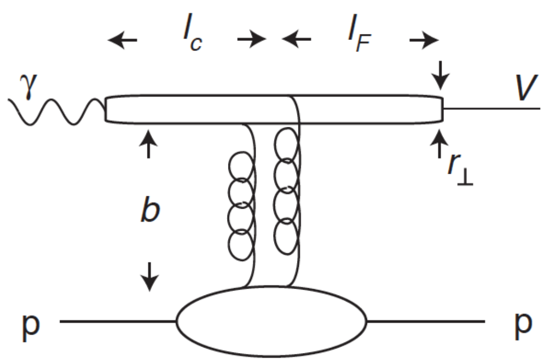

Figure 3: VMD picture of a vector meson photoproduction (diagram is from [1]).

$$
\begin{aligned}
b &\approx \frac{1}{\sqrt{-t}} \approx 0.2\ fm, \\
r_\perp &\approx \frac{1}{m_c} = 0.13\ fm, \\
l_F &\approx \frac{2E_{J/\psi}}{2m_c(m_{\psi'} - m_{J/\psi})} \approx 1-2\ fm.
\end{aligned}
\tag{3}
$$

Small b and $r_\perp$ create conditions where the J/ψ photoproduction can be used as an effective tool to study the nucleon form factor of a gluonic operator, providing unique information on the non-perturbative gluon fields in the nucleon. In order to have an elastic scattering (where the nucleon stays intact), partons in the nucleon must share the large transferred momentum to the $\bar{c}c$ pair and must be in a compact Fock state. The large momentum transfer can lead to the dominance of multi-gluon exchange reactions, allowing a charmonium bound state formation [34].

As multi-gluon exchange is the dominant contribution to the J/ψ photoproduction, the quark content of the target nucleon does not play a role and we expect that the cross-section value, and its dependence on the transferred momentum and the beam energy should be the same for production off the proton and off the neutron. Similarly, charmonium bound states should exist in both isospin states. In this proposal we will extend proton gluonic form-factor studies of [17, 18] to bound nucleons, proton and neutron in the deuteron, and will search for isospin parters of the LHCb pentaquarks $P_c^0(4380)$ and $P_c^0(4450)$, by studying the invariant-mass spectrum $M(J/\psi n)$.

2.3 Coherent J/ψ Photoproduction off the Deuteron

At high energy, J/ψ photoproduction is well understood and can be described by generalized parton distributions (GPDs) [15]. While the possibility of a small component of intrinsic charm in nucleons (and nuclei) has not yet been completely ruled out, it can for all practical purposes be neglected. Thus, the process can be described as a fluctuation of the photon into a $c\bar{c}$ dipole, which then couples to the gluon field of the nucleon by a two-gluon exchange (one gluon from each quark). This makes charmonium production sensitive to the gluon distribution in the nucleon, and in particular the nucleon gluon GPD, which parametrizes further soft gluon exchanges within the nucleon (it is thus not a model assuming that a certain number of gluons is exchanged). Accessing the gluon GPD relies on factorization of the process into a hard and a soft part, the former described by a hard scattering and the latter parametrized by the GPD. The hard scale of the former is set by the $q\bar{q}$ distance. For light-quark systems, this is determined by the value of Q^2, which sets an initial scale, and an assumption that the distance traveled is small compared to the coherence length. This allows the squeezed meson to exit the nucleon (or nucleus) while the medium is still transparent, thereby ensuring dominance of the handbag diagram. However, in heavy quarkonia, the color dipole size is small even for the fully formed meson, making the process perturbative at all values of Q^2. Naively, the equivalent value is then given by M^2. For charmonium, the actual value is a little lower, but nevertheless ensures factorization for all values of Q^2, including photoproduction.

At high energy (s), the longitudinal momentum transfer ($t \approx p_T^2$) and t_{min} are small, implying that the momentum difference between the exchanged gluons is small. In the language of GPDs, this corresponds to a small skewness (difference in x between the initial and final states). If the skewness is large, which is necessary to create a large longitudinal momentum transfer, the process can still formally be described by GPDs, but the connection to a transverse spatial image becomes very model-dependent (the distribution in impact-parameter space is no longer simply a Fourier transform of the measured t-distribution). At low energy, where t_{min} and the skewness are large, the process can be described in terms of a gluonic form factor, allowing some spatial information to be recovered, but higher photon energies are clearly preferable in terms of physics interpretation. For coherent production off the deuteron, t_{min} ranges from 3.31 (GeV/c)^2 at threshold (5.66 GeV photon energy) to 0.26 (GeV/c)^2 at 11 GeV. Fortunately, the rising cross section means that most of the data will be collected at the highest energies, allowing us to measure a t-distribution between 0.3 and 1 (GeV/c)^2, which is well suited to a GPD interpretation. For coherent production off the deuteron, the cross section is also suppressed by the deuteron form factor. The magnitude of this suppression is thus higher at larger values of t, making the high-s, low-t range the ideal kinematics for this measurement.

A comparison of the transverse spatial gluon distribution in the proton and the deuteron, which is the least dense nucleus, would provide a first glimpse into the nuclear gluon distribution a decade before the advent of the Electron-Ion Collider (EIC). At the EIC, coherent diffraction on nuclei (in particular using heavy-flavor production), is one of the key measurements, as it makes it possible to map out the spatial distribution of gluons in nuclei (while incoherent production tells us about the fluctuations in this distribution).

The proposed CLAS12 RGB measurement will be the first 12 GeV experiment able to measure coherent J/ψ production on the deuteron. Unfortunately, the cross section is not well known, and rate estimates suggest anything from a few events per (PAC) day to a few days per event. In an optimistic scenario, the RGB data would be able to provide a first measurement of the t-distribution, while in a pessimistic one, they would provide a reliable rate estimate for future experiments. In either case, the data will be very important for measuring the gluon distribution in nuclei at the 12-GeV JLab. It should also be noted that RGB will also provide data on coherent ϕ electroproduction on the deuteron. However, due to the low mass of the strange quark, the ϕ meson needs to be produced at very high Q^2 in order to ensure factorization, which greatly reduces the rate and limits the accessible kinematics at 12-GeV JLab energies (in a non-trivial way compared to simply needing high photon energies in the case of the J/ψ. At the EIC, measuring ϕ production on nuclei is interesting since it allows tuning of the dipole size by varying the Q^2, but due to the kinematic restrictions, this is not a desirable feature at 12 GeV. The ϕ also makes interpretation more complicated since the strangeness content of nucleons and nuclei cannot be neglected. Still, since no high-Q^2 ϕ electroproduction data exist on the deuteron in JLab 12-GeV kinematics, an after-the-fact data analysis may be of interest. But we are not pursuing it as the primary means of probing nuclear glue.

3 CLAS12 and Experimental Capabilities

The proposed program will make use of the beam time allocated for the current Run-Group B proposals with 11-GeV electron beam and a luminosity of 10^{35} $\mathrm{s}^{-1}\mathrm{cm}^{-2}$. Thus, it will be carried out using the baseline equipment in Hall B as well as the Central Neutron Detector (CND) and the Forward Tagger (FT). We will make use of the CLAS12 capabilities to detect and identify charged hadrons in the LS-polar-angle range from 5° to 125°, to detect and identify neutrons in the Forward Electromagnetic Calorimeter (FEC) in the LS polar-angle range from 5° to 40°, to detect neutrons in the CND at angles $40^\circ - 120^\circ$, and to detect and identify electrons and positrons in the LS polar-angle range from 5° to 40° in the forward detector (primarily the High-Threshold Cherenkov Counter, HTCC). The studies will be done by detecting the electron-positron pair from the J/ψ decay and will make use of the standard electron trigger in CLAS12. We will need an additional trigger for charged particles in opposite sectors, to capture the muonic decay of J/ψ, that will add 20% to the trigger rate. We will negotiate with the rest of Run Group B the inclusion of such trigger during data taking.

Due to the multiple final-state particles in the reactions of interest, the corresponding yields will be extracted from different event topologies as described below. The kinematic ranges of the outgoing particles were obtained by using a phase-space event generator, where each elementary process, namely $\gamma N \to J/\psi N$, $J/\psi N \to J/\psi N$, and $\gamma d \to J/\psi d$ was generated according to its own phase space. The Fermi momentum of the nucleons in the deuteron was randomly generated according to the Paris potential. The spectator nucleon was always generated on its mass shell, while the mass of the target nucleon was such that the sum of the total energies of the two nucleons yielded the deuteron rest mass.

3.1 Final-State Interactions in Incoherent J/ψ Photoproduction off Deuteron

In order to access the $J/\psi N$ interaction cross section, we need to be able to detect the outgoing particles produced in the mechanism depicted in the bottom panel of Fig. 1, where J/ψ is produced in the elementary reaction $\gamma N_{1,bound} \to J/\psi N_1$ in a first step and then it re-scatters off the other nucleon via the reaction $J/\psi N_{2,bound} \to J/\psi N_2$. Here the label 1(2) of the scattered nucleon is only introduced in order to distinguish between the nucleon involved in the first step from the nucleon involved in the second step of the FSI. The final-state particles in this two-step mechanism are exactly the same as in the quasi-free J/ψ photoproduction off the bound nucleon. In each case, we are looking at incoherent photoproduction $\gamma d \to J/\psi pn$. However in quasi-free production, one of the outgoing nucleons is a low-momentum nucleon, while in FSI, both the outgoing nucleons carry high momenta. While the extraction of the $J/\psi N$ cross section from FSI yields does require theoretical input, *i.e.* it will be model dependent, since experimentally it is not possible to kinematically separate between various FSI leading to the final state of interest, it is important to assess the possibility to separate between quasi-free and FSI events.

The kinematics of the outgoing particles in case of a two-step mechanism involving $J/\psi N$ rescattering is shown in Fig. 4. The top two panels of Fig. 4 show that the two final-state nucleons produced in the FSI of interest have momenta in the range of up to 5–6 GeV/c. While N_1 scatters predominantly at LS polar angles below 50°, N_2 scatters over a much broader angular range, up to 160° [1]. The J/ψ kinematic distribution (bottom left panel of Fig. 4) also shows an interesting trend. While the momentum range is similar to the one for the QF mechanism, the angular range of a re-scattered J/ψ is about two times wider, *i.e.* J/ψ scattered at angles above 10° could not have been produced in a QF production or in a NN rescattering, but only in a $J/\psi N$ rescattering. The latter provides some experimental means to obtain a FSI interaction sample dominated by $J/\psi N$ rescattering. These distributions, coupled with the CLAS12 acceptance for protons and neutrons, suggest that the FSI of interest will be measured in the following ways:

[1] In fact the nucleon produced in the second-step elastic $J/\psi N$ scattering, covers the full LS polar angle from 0° to 180°, which is a characteristic of elastic scattering. The actual angular range shown in the figure is narrower due to the limited CLAS12 angular acceptance for e^+, e^-, and N_1.

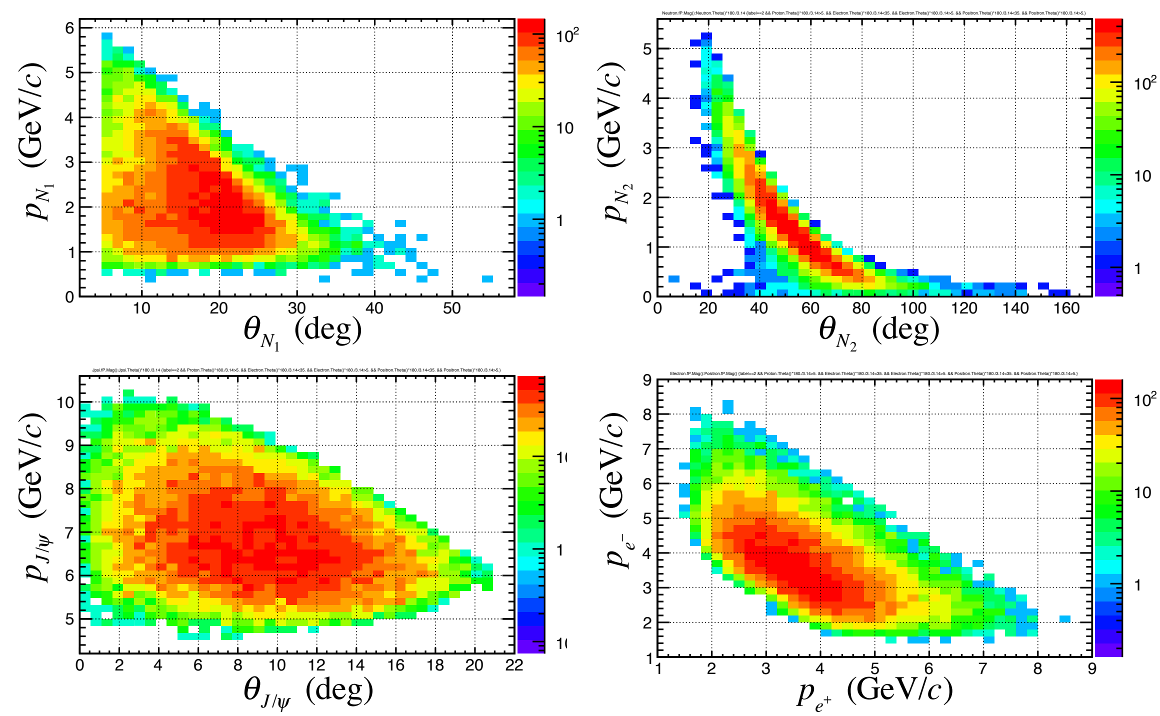

Figure 4: Top Left: Momentum versus polar angle in lab system of the nucleon N_1 produced in the first step of the FSI of interest. Top Right: Momentum versus polar angle in lab system of the nucleon N_2 produced in the second step of the FSI of interest. Bottom Left: Momentum versus polar angle in lab system of the J/ψ produced in the FSI of interest. Bottom Right: The kinematic correlation p_{e^-} vs. p_{e^+}. All distributions are produced by taking into account that the e^+e^- will be detected in the limited polar angular range of $(5^\circ,\ 35^\circ)$ and that the final state proton will be detected at polar angles above 5°. The distributions are produced with beam-photon energies from threshold up to 11 GeV.

1. Untagged Real Photoproduction: All final state particles are detected and the beam photon is reconstructed from four-momentum conservation (scattered electron is very forward and not detected. This approach will yield access predominantly to $J\psi p$ rescattering, as the neutron produced in the first step is predominantly forward scattered and will be detected in the FEC, while the large CLAS12 acceptance for protons will allow to detect the protons produced in the second step over the full CLAS12 LS polar-angle range. The momenta of both nucleons fit very well with the nominal CLAS12 specifications for efficient neutron and proton PID.

   This technique will yield a more limited yield for $J\psi n$ rescattering, due to the fact that a significant number of final-state neutrons will scatter at angles above 35°. The momenta of these neutrons are up to 3 GeV/c. While the central-neutron detector can detect neutrons scattered at angles above 40°, (a) it provides a good n/γ separation for neutrons below 1 GeV/c, which means an increased background in our yields of events with neutrons having momenta between 1 GeV/c and 3 GeV/c, and (b) it has a neutron detection efficiency of 10% – 15%. The experiment itself will provide the full information about the level of backgrounds due to poor neutron identification in the central neutron detector above 1 GeV/c and will allow for the development of refined techniques for background reduction in the offline data analysis.

2. Quasi-real Photoproduction: This approach makes use of detecting a small-angle scattered electron in the forward tagger, which allows to reconstruct the four-momentum of the low-Q^2 quasi-real photon. With the kinematics of the beam photon known, one of the final-state particles can be undetected and the reaction identified by the missing-mass technique.

   There are two event topologies, which will be explored with this technique: (a) $\gamma d \to pJ/\psi X$, where $X \equiv n$, and (b) $\gamma d \to nJ/\psi X$, where $X \equiv p$. The first event topology will provide more events in the $J\psi n$ rescattering sample and may turn out to be the main way to access this yield. The second topology will provide more events to the $J\psi p$ rescattering sample and can also be used for systematic checks of the extracted cross sections as the CLAS acceptance for the topologies of untagged real photoproduction and quasi-real photoproduction will be very different. This topology also allows kinematic access to forward scattered protons, which was shown in [13] to be advantageous for the $J/\psi N$ interaction study.

In order to obtain an idea of the expected counting rates, we implemented the model of [3] in an event generator. Our cross section studies show that the quasi-free J/ψ production dominates by many orders of magnitude at low "spectator" momenta (with "spectator" we denote the nucleon off which the meson rescatters in the second step of the reaction). The most beneficial kinematics to measure $J/\psi N$ rescattering cross section is at "spectator" momenta $\geq$ 600 MeV/c, where rescattering mechanisms dominate. In order to enhance the sensitivity to $J/\psi N$ rescattering over NN rescaterring, we will narrow the kinematics to forward neutron angles relative to the three-momentum transfer to the pn system, as suggested by Fig. 2.

Overall, we expect the total yield of rescattering events (events with "spectator" momentum $\geq$ 600 MeV/c) to be below 10% of the total quasi-free yield, depending on the value of the total $J/\psi N$ cross section. If the total $J/\psi N$ cross section is of the order of 15 mb, we will be able to observe it. A total cross section of the order of a few mb will be much more challenging to measure and in such a possible scenario, we will be able to estimate an upper limit. In all cases, the experimental estimates will bear a model-dependent systematic uncertainty due to the use of a model for the high-momentum tail of the deuteron wave function and the NN final-state interactions, which both contribute to the event yield at high "spectator" momentum. In any case, this measurement will be the very first FSI measurement of $J/\psi N$ close to threshold and will provide benchmark data for the $J/\psi N$ studies.

3.2 Quasi-free J/ψ photoproduction off the Bound Neutron

3.2.1 Kinematics of J/ψ photoproduction off the Bound Neutron

We studied quasi-free production of J/ψ from bound proton and neutron in deuterium with 11 GeV electrons using the reaction

$$e^- d \to J/\psi N'(e' N_s). \tag{4}$$

Here N' denotes the strike nucleon, while N_s is the undetected spectator nucleon. The e' is the scattered electron and the J/ψ is identified through its e^+e^- or $\mu^+\mu^-$ decay. Simulations were done for both, the bound proton and the bound neutron in deuterium with realistic Fermi momentum smearing using the Bonn potential for the deuteron wave function. Kinematical distributions and acceptances were compared with the results of simulations for production on hydrogen. Details of the simulations are described in [17]. The CLAS12 detector response was simulated using the Fast Monte-Carlo code (as in the previous CLAS12 J/ψ proposals). For neutron detection, the efficiency was extracted by using the parametrization of the neutron detection efficiency of the CLAS12 forward calorimeter from [35]. The neutron momentum was calculated from time of flight assuming $\sigma_t = 0.5$ ns time resolution of the calorimeter.

The simulation did not account for final-state interactions; production was assumed to be elastic on one of the bound nucleons, while the other nucleon escapes as a spectator. We show the momentum distributions of the strike (red) and spectator (blue) nucleons in Fig. 5. The strike nucleon, as in case of the recoil proton in J/ψ production on hydrogen, scatters forward and can be detected in the CLAS12 forward detector (FD). The spectator is released uniformly in LS polar angle with momentum largely $<$ 0.3 GeV/c (Fermi momentum) and will escape detection in CLAS12.

The detection kinematics range and efficiency for protons are described in [17, 18]. In Fig. 6 ϕ vs θ, and θ vs. momentum are shown for strike neutrons. The generated spectrum

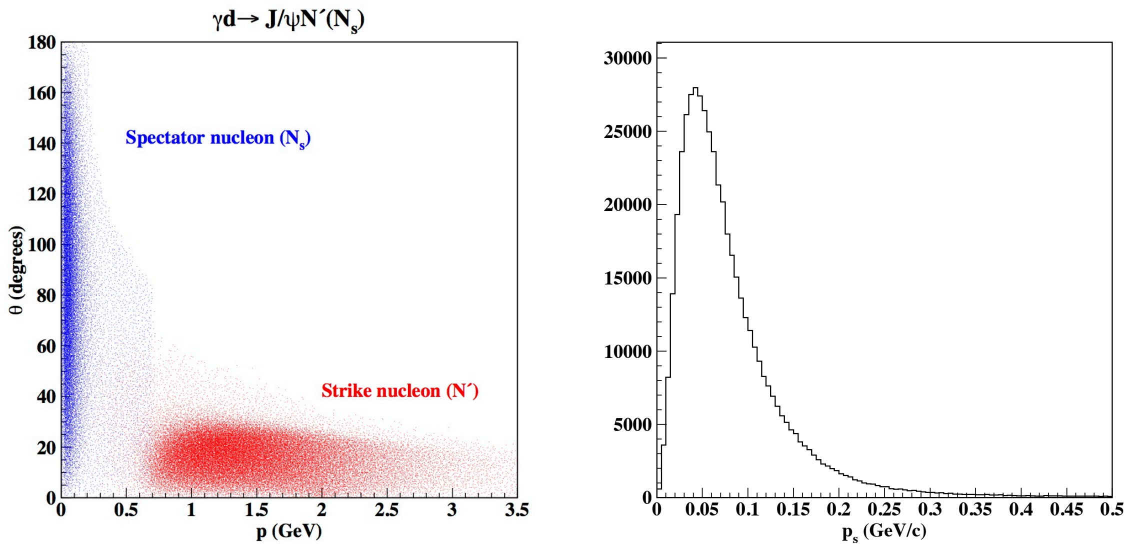

Figure 5: Left: scattering angle vs. momentum of nucleons, strike - red, and spectator - blue, in the quasi-free production of J/ψ off the deuteron in quasi-free kinematics. Right: spectator momentum distribution.

is in green, the red areas are for detected neutrons in the CLAS12 forward calorimeters. The detection efficiency for strike neutron as a function of transferred momentum squared t and the photon energy E_γ is shown in the left graph of Fig. 7.

On the right graph of Fig. 7 the ratio of the efficiencies for neutron and proton (from production on hydrogen) detection is shown in the kinematical range of the experiment. The neutron detection efficiency is of the same order as for protons from the J/ψ production on hydrogen. Therefore we can assume that the J/ψ production rate in quasi-free scattering off the bound neutron (and also the bound proton) in electron-deuterium scattering will be similar as in the reaction on hydrogen.

Important kinematical parameters for identifying the quasi-free J/ψ production on a bound nucleon in quasi-real photoproduction are the transverse momentum (p_T), and the missing mass squared distributions of the detected particles. Here, "transverse" denotes a direction perpendicular to the direction of the primary electron beam. Let us consider J/ψ production off the bound nucleon N. We will detect only the scattered nucleon N' and J/ψ , and make use of the fact that the direction and the momentum of the primary electron beam, e, are known. Let us denote the spectator nucleon with N_{sp}. Then the mass squared, m_X^2 (Missing Mass^2), of the missing state X in the reaction $e + N_{sp} + N \to X + N' + J/\psi + N_{sp}$ can be

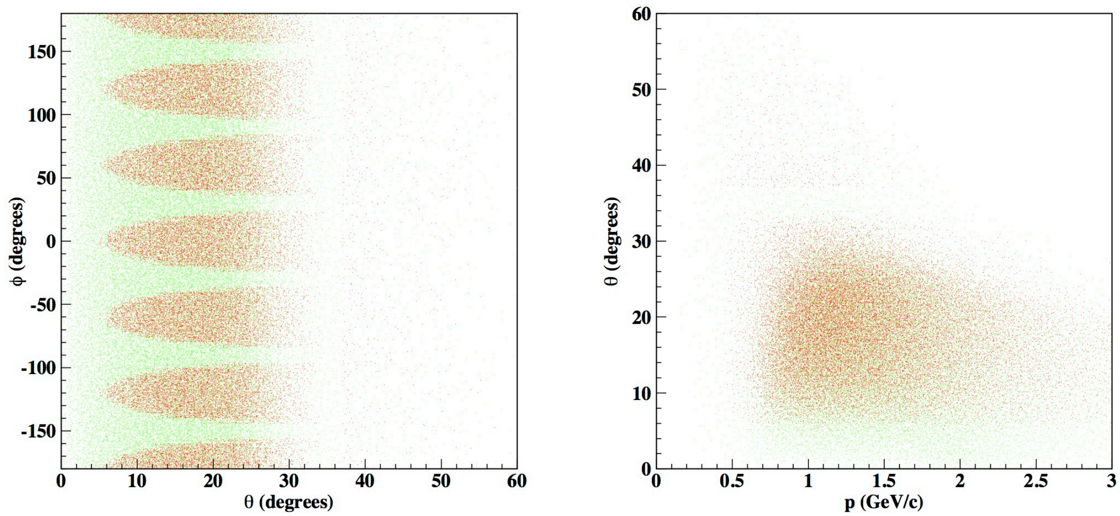

Figure 6: Phase space of strike neutrons in quasi-free J/ψ photoproduction off the bound neutron. Left: LS azimuthal angle ϕ vs. LS polar angle θ. Right: LS θ vs. momentum. The green area shows all final-state neutrons. The red points represent neutrons detected in the forward calorimeters.

found as:

$$m_X^2 = (\tilde{p}_e + \tilde{p}_N - \tilde{p}'_N - \tilde{p}_{J/\psi})^2, \tag{5}$$

where $\tilde{p}$ denotes a four-momentum vector and the subscript of $\tilde{p}$ denotes the corresponding particle. The transverse momentum, Missing p_T, of the missing state X can be found from linear-momentum conservation:

$$\vec{p}_{X_T} = \vec{p}_{e_T} + \vec{p}_{N_T} - \vec{p}_{N'_T} - \vec{p}_{J/\psi}. \tag{6}$$

We assume that the target nucleon is at rest, *i.e.*, $\tilde{p}_N = (0, 0, 0, m_N)$. This is a reasonable assumption since the typical nucleon momenta in the deuteron are much smaller than the momenta of the scattered particles. Since we assume that N_{sp} does not participate in the reaction, its 4-momentum vector does not enter in the equations of interest. The primary electron beam has $p_{e_T} = 0$. Also, we will select specifically events in which the scattered electron e' is not detected, *i.e.*, for our event sample, e' scatters at a small angle and in the forward hole of CLAS12. This restriction means that the $p_{e'_T}$ is expected to be very small compared to the momenta of the other particles involved in the reaction. We then set $\vec{p}_N = 0$

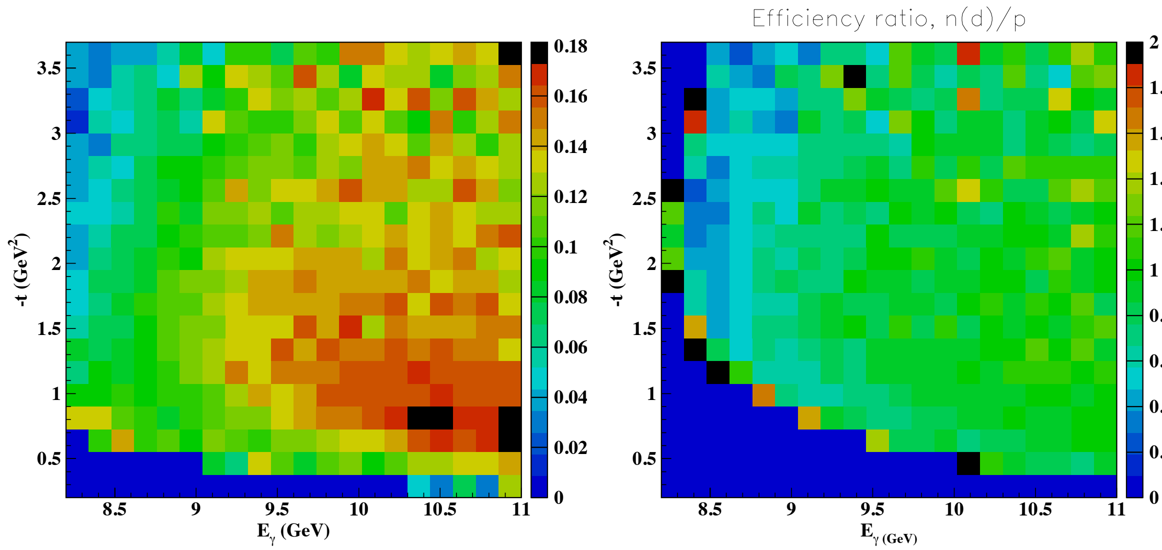

Figure 7: Left: neutron detection efficiency in the space of t (the transferred momentum) and E_γ (the photon beam energy). Right: ratio of the efficiencies for neutron and proton (from J/ψ production on hydrogen).

and the above equations become:

$$m_X^2 = (\tilde{p}'_e + \tilde{p}_N - \tilde{p}'_N - \tilde{p}_J/\psi)^2 \tag{7}$$

$$p_{X_T} = p_{N'_T} + p_{J/\psi_T}. \tag{8}$$

Eq. 7 is used to make sure that m_X^2 is consistent with the rest mass of the scattered electron for the reaction of interest, whereas Eq. 8 is used to make sure that the transverse momentum of the scattered electron is zero. Then, the photon beam energy can be determined as $E_\gamma = p_{N'_z} + p_{J/\psi_z}$, where the Z axis is parallel to the direction of the primary electron beam.

Figure 8 shows a comparison of the event distributions over Missing p_T (left panel) and Missing Mass^2 (right panel) for J/ψ quasi-free production with 11 GeV electrons off the bound proton (blue) and off the neutron (red) in deuteron and those for J/ψ production with 11 GeV electrons off the free proton (black). The kinematical dependence on t and E_γ in all three reactions is the same. While due to Fermi-momentum smearing (we assume the bound nucleon to be at rest), the transverse momentum and the missing-mass squared distributions are wider for scattering off bound nucleons than for scattering off free protons, nevertheless they are still reasonably narrow and distinct for selection of the quasi-feee reaction. Most importantly, there is a very little difference between the bound proton and neutron kinematics, which will ensure small systematical uncertainties when comparing the J/ψ production off the bound proton to that off the bound neutron.

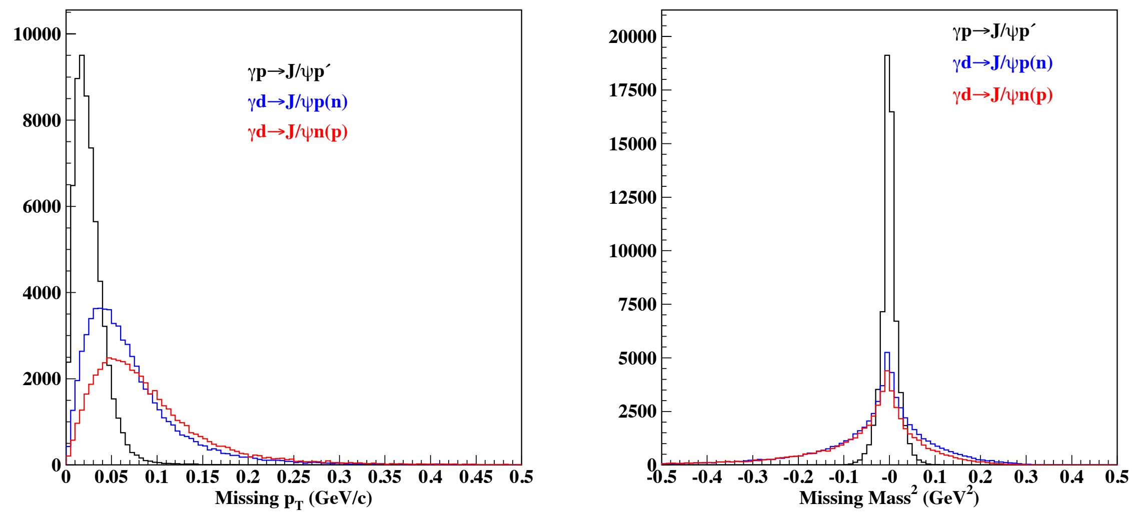

Figure 8: Missing transverse momentum and missing-mass squared distributions for J/ψ production in the reactions; $ep \to J/\psi p'(e')$ and $eN \to J/\psi N'(e')$, where in the latter N is either the proton or the neutron in the deuteron with Fermi-momentum defined by a model using Bonn potential, and we assume that the second nucleon escapes as a spectator. Curves correspond to production on hydrogen (black), on the proton (blue) and on the neutron (red) in the deuteron.

The pentaquark states will be identified in the invariant-mass distribution of J/ψ and the nucleon. The invariant-mass resolution will not depend on Fermi momentum, but will be somewhat worse for the neutral pentaquarks due to the worse neutron-momentum resolution (defined by time resolution of the calorimeter) compared to the proton momentum resolution. In Fig. 9 the expected invariant-mass resolution (left) and the detector acceptance (right) for the ne^+e^- system are presented. The invariant-mass resolution is still smaller than the width of the narrow LHCb pentaquark, which is 40 MeV. The vertical line on the acceptance graph shows where we expect the pentaquark states. The detection efficiency is of the same order as for the proton case in the production on hydrogen (as it already was stressed above) and, therefore, we expect the same J/ψ and pentaquark yield on the bound neutron and bound proton.

In summary, we expect J/ψ production in quasi-free production off nucleons in deu-

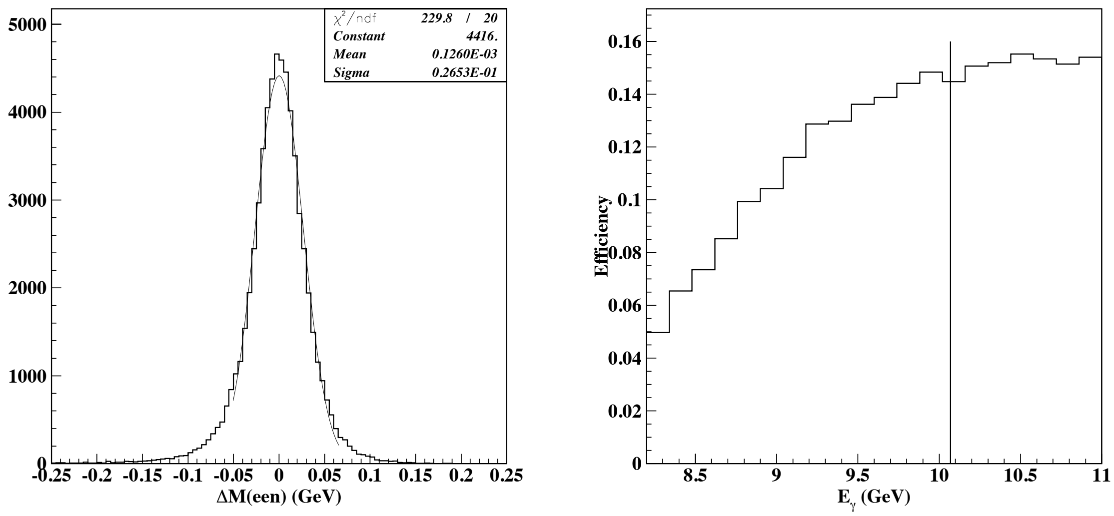

Figure 9: The invariant mass resolution of ne^+e^- system (left) for 500ps time resolution of ECal for neutron detection, and the acceptance vs. photon energy plot for ne^+e^- system (right). The vertical line on right graph is where we expect to see pentaquark states.

terium to be similar in cross section to the production off the free proton. Studies with the CLAS12 Fast Monte Carlo simulation, using the same event generator that has been used for [17] show that detection efficiencies for detecting scattered proton and scattered neutron in J/ψ photoproduction are of the same order. Therefore, we conclude that the J/ψ production rate on the deuteron target in the quasi-free scattering off bound nucleons, should be at the same order as presented in [17, 18].

3.2.2 Estimate of the pentaquark yield

The expected rates for J/ψ production and the statistical precision for measuring t- and energy dependences have been detailed in the E12-12-001 proposal [17]. Since the detection efficiencies for protons and neutrons in the kinematics of J/ψ production are very similar to each other, the J/ψ yield in quasi-free production on a nucleon in deuterium will be of the same order. We expect (after correcting for current tracking efficiency of CLAS12 Forward Detector) about 15 J/ψ 's per day detected in e^+e^- decay mode for each the bound proton and bound neutron. This estimate expects that running luminosity will be 10^{35} cm^{-2} sec^{-1} on deuteron ($\times 2$ per nucleon). This is a reasonable assumption from the point of view of the background in region 1 drift chambers.

If we add also J/ψ detection via its di-muon decay, $J/\psi \to \mu^+\mu^-$, then the rates will be double. The muon trigger was implemented in the Run Group A experiment in 2018. The muons were identified by the preshower calorimeter (PCAL) and electromagnetic calorimeter (ECAL) by demanding minimum-ionizing-particle (MIP) signal in both detectors. The pion background was rejected by a factor of 2 giving the final factor of 4 for the negative and positive particles all together. The remaining pion background was estimated to be at the same level as the J/ψ signal in the region of the invariant mass near 3.1 GeV/c^2. In addition, the coincidence of two charged particles was required in two opposite CLAS12 sectors as is supposed to be for the decay of $J/\psi \to \mu^+\mu^-$.

Here we present the expected rates for pentaquarks ($E_\gamma \simeq 10$ GeV) based on the cross-section formalism presented in [21]. In order to calculate the expected rates, one should also take into account a $BR(J/\psi \to e^+e^-) \simeq 0.06$ and the detector efficiency (acceptance) of $\epsilon \simeq 0.1$ in the pentaquark mass range. The total number of events in CLAS12 for the reaction $\gamma n \to P_c \to J/\psi n$, $J/\psi \to e^+e^-$ was estimated as:

$$N(P_c) = \int \sigma(W)\frac{dL_\gamma}{dW}\,\epsilon\; dW \cdot Br(J/\psi \to e^+e^-) = 0.5 \int \sigma(W)dW \text{ events/nb/MeV/day} \quad (9)$$

where $\frac{dL_\gamma}{dW} = 10^{30}$ events/cm^2/MeV/s=10^{-3} events/nb/MeV/s is the CLAS12 photon luminosity per $\Delta W = 1$ MeV bin at nominal electron-neutron luminosity $L_{en} = 10^{35}$ cm^{-2} sec^{-1}. Detection of J/ψ in the $\mu^+\mu^-$-decay mode will double the statistics because the $BR(J/\psi \to e^+e^-) = BR(J/\psi \to \mu^+\mu^-)$.

The pentaquark yield for one day at luminosity $L_{en} = 10^{35}$ cm^{-2} sec^{-1} is presented in Table 1 for two pentaquark states and two values of the predicted cross sections [21] assuming $Br(P_c \to J/\psi n) = 1\%$, which is very conservative. In Fig. 10 we show the dependence of the

Table 1: Estimated number of detected pentaquarks per day. The numbers are obtained with a realistic tracking efficiency for a 3-particle final state.

	Minimum - Maximum
$P_c(4380)$	31 - 975
$P_c(4450)$	45 - 1430

J/ψ photoproduction cross section on E_γ with and without $P_c(4450)$ as well as the expected corresponding measured cross-section values. The projected results were estimated for a 30-day running off a free proton target at the same conditions as for running off a deuteron target and assuming 100% tracking efficiency. The CLAS12 realistic tracking efficiency for 3 detected particles is about 65%. Thus, the estimates in the figure correspond to ~ 50 days of running with realistic tracking efficiency. Data collected over the allocated 80 days of beam time for RGB will reduce the statistical uncertainties shown in the figure. The figure demonstrates that the expected data sample will have sufficient statistical significance to clearly identify if there is a pentaquark signal in the energy dependence of the total photoproduction cross section.

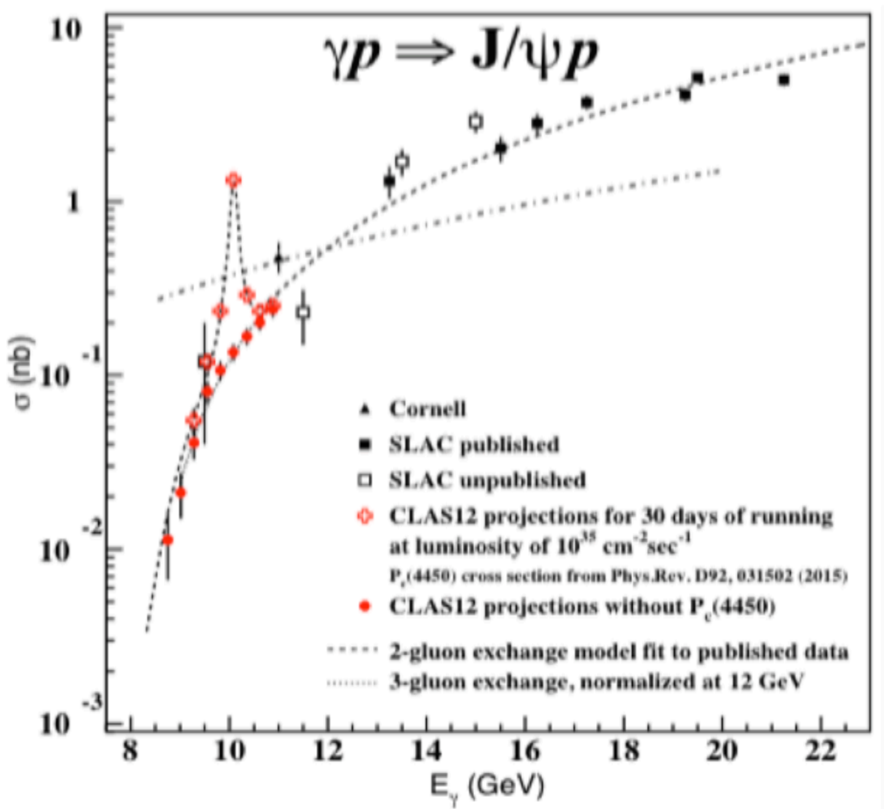

Figure 10: Photon-energy dependence of the J/ψ photoproduction cross section off the free proton at standard running conditions considered in this proposal and 100% tracking efficiency. Since the expected counting rates in quasi-free photoproduction off deuteron are comparable to the counting rates expected off a free proton, the figure is representative of the statistical significance of the proposed measurement off the bound proton. The resolution for production off the bound neutron will be lower but still better than the width of 40 MeV of the LHCb pentaquark. The red symbols show the expected experimental cross-section values with and without $P_c(4450)$. The pentaquark cross section was estimated in [21] with branching ratio $BR(P_c(4450) \rightarrow J/\psi{+}p) = 0.01$. The resolution and the counting rates are sufficient to clearly identify a pentaquark signal, for both cases of the estimated numbers of detected pentaquarks shown in Table 1. Figure from J. Newton.

3.3 Coherent J/ψ photoproduction off deuteron

Figure 11 shows the kinematics of the scattered deuteron, J/ψ, and the electron (positron) from the meson decay for photon energies from threshold up to 11 GeV. One can see that the

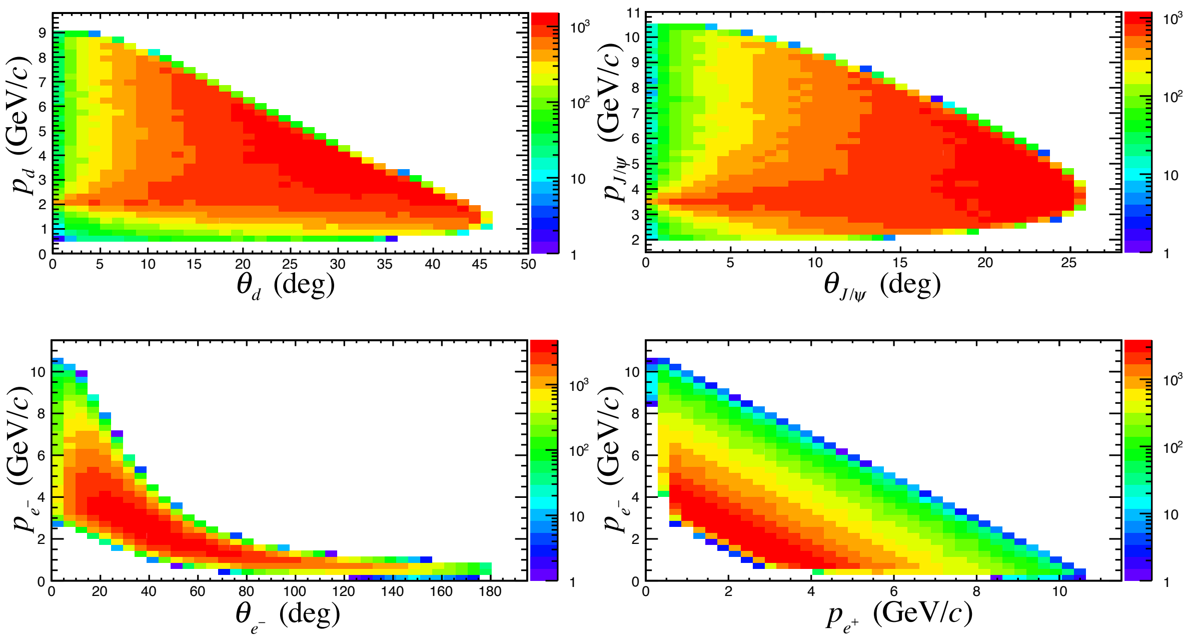

Figure 11: Top Left: Momentum versus LS polar scattering angle in lab system of the scattered deuteron in the reaction $\gamma d \to J/\psi d$ for photon energies from threshold up to 11 GeV. Top Right: Momentum versus LS polar scattering angle in lab system of the scattered J/ψ in the reaction $\gamma d \to J/\psi d$ for photon energies from threshold up to 11 GeV. Bottom Left: Momentum versus LS polar scattering angle in lab system of the electron from the decay $J/\psi \to e^+e^-$. The kinematic correlation p vs. θ of the decay positron is exactly the same as the one of the electron. Bottom Right: The kinematic correlation p_{e^-} vs. p_{e^+} within the geometrical acceptance of the forward High-Threshold Cherenkov Counter and the Forward Electromagnetic Calorimeter.

vector meson produced in this process covers a wider LS polar angular range than the range covered in photoproduction off the nucleon. However, J/ψ produced in FSI also covers similar wider range. Given that, it is clear that the yield extraction for this process must be based on the detection of the scattered deuteron. The top left panel of Fig. 11 shows that the scattered deuterons span a momentum range from 0.5 GeV/c up to 9. GeV/c and LS polar angles up to 45°.

Although, the CLAS capabilities, deuteron form factor, and reaction dynamics will limit these kinematics ranges, we expect to be able to identify most of the final-state deuterons. With the deuteron and the decay electron and positron pair from the J/ψ decay detected, we will identify the meson via invariant mass, and reconstruct the photon via four-momentum conservation. In this case, the scattered beam electron moves at very forward angles and is not detected (either in CLAS or in the forward tagger).

The biggest challenge for the study of the coherent production close to threshold is the cross section suppression due to the deuteron form factor, which decreases rapidly as t increases. While the J/ψ production on the deuteron would be increased by about a factor of four compared to the free-proton [2], the probability that the deuteron remains intact after absorbing a momentum transfer t is much smaller than the probability for a proton to do so after absorbing the same momentum transfer. Thus, we expect reduced counting rates compared to the ones for J/ψ production on the free proton. However, it is worth noting that the emphasis for coherent production is on higher s, where t-values in the 0.3-1 $(\mathrm{GeV}/c)^2$ range can be reached. Based on the ratio of the cross sections for coherent ϕ-meson production off the deuteron and off the free proton from CLAS and on the J/ψ cross-section on the proton, we estimate that the coherent rate will be around one event per 2–3 PAC days if we include both electron and muon decay branches of the J/ψ. The uncertainty on this estimate is large - but this is one of the reasons why it is so important to actually measure this process.

3.4 Compatibility with Run Group B

The proposed measurements make use of the CLAS12 baseline detector and are compatible with the running configuration of Run Group B. In addition, during RGB data taking several non-baseline systems will be operated, namely the forward tagger (FT), the central neutron detector (CND), the Ring Imaging Cherenkov Detector (RICH), and the Back-Angle Neutron Detector (BAND). We will make use of the forward tagger, which has already been operated during Run Group A data taking and is an established detector component, and will explore the opportunity to make use of the CND. Neither, the FT or the CND, are critical for the proposed measurements and their operation is expected to slightly increase our counting rates. For example, the use of the FT will add up to 10% more events. Our measurements are independent of RICH and BAND.

RGB plans to take data with 100% torus field during all of the allocated beam time. During about 75% of the running, the field will be "negative", *i.e.*, negatively-charged particles are inbending. During the remaining 25% of the running, the torus field will be "positive", *i.e.*, negatively-charged particles will be outbending. This torus field configuration is the same as used during Run Group A, satisfies the experimental requirements of the proposed measure-

[2] In the impulse approximation of the coherent J/ψ photoproduction off deuteron, the invariant cross section is approximately equal to four times the product of the invariant cross section of J/ψ photoproduction off the nucleon and the deuteron form factor.

ments, and is compatible with our rate estimates. It is worth noting that the measurement of the quasi-free J/Ψ photoproduction off the bound neutron is independent of the direction of the torus field since the neutron acceptance is field-independent and the acceptance for detection of the electro-positron, or muon-antimuon, pair from the J/Ψ decay is the same for either direction of the field.

In addition to the standard trigger for RGB, we will make use of a muon trigger, as described in Section 3.2.2, which will be negotiated with the other experiments in the run group. Preliminary discussions suggest that there is no strong opposition to implementing such a trigger during the RGB data taking. The muon trigger will increase the expected rates reported here by a factor of 2.

References

[1] S.J. Brodsky, E. Chudakov, P. Hoyer, and J.M. Laget, Phys. Lett. B 498, 23 (2001).

[2] J.M. Laget and R. Mendez-Galain, Nucl. Phys. A 581, 397 (1995).

[3] A.J. Freese and M.M. Sargsian, Phys. Rev. C 88, 044604 (2013).

[4] B.Knapp, W.-Y. Lee, P. Leung, S.D. Smith, A. Wijangco *et al.*, Phys. Rev. Lett. 34, 1040 (1975).

[5] R.L. Anderson *et al.*, Phys. Rev. Lett 38, 263 (1977).

[6] D. Kharzeev and H. Satz, Phys. Rev. Lett B334, 155 (1994).

[7] A. Sibirtsev and M.B. Voloshin, Phys. Rev. D 71, 076005 (2005).

[8] M. Luke, A. V. Manohar, and M. J. Savage, Phys. Lett. B 288, 355 (1992).

[9] S. J. Brodsky, and G. A. Miller, Phys. Lett. B 412, 125 (1997).

[10] B. Alessandro et al., Eur. Phys. J. C 48, 329 (2006).

[11] T. Matsui and H. Satz, Phys. Lett. B 178, 416 (1986).

[12] O. Lakhina amd E. S. Swanson, Phys. Lett. B 582, 172 (2004).

[13] , J.J. Wu and T.-S. H. Lee, Phys. Rev. C 88, 015205 (2013).

[14] , G.T. Howell and G.A. Miller, Phys. Rev C 88, 015204 (2013).

[15] L. Frankfurt and M. Strikman, Phys. Rev. D 66, 031502(R), 031502 (2002).

[16] Z.-E. Meziani *et al.*, https://www.jlab.org/exp_prog/proposals/16/PR12-12-006.pdf.

[17] S. Stepanyan *et al.*, https://www.jlab.org/exp_prog/proposals/12/PR12-12-001.pdf.

[18] S. Stepanyan *et al.*, https://www.jlab.org/exp_prog/proposals/17/E12-12-001A.pdf.

[19] Z.-E. Meziani *et al.*, https://www.jlab.org/exp_prog/proposals/16/PR12-16-007.pdf.

[20] R. Aaij *et al.* [LHCb Collaboration], Phys. Rev. Lett. **115**, 072001 (2015), arXiv:1507.03414 [hep-ex].

[21] V. Kubarovsky and M.B. Voloshin, Phys. Rev. D **92** 3, 031502, 2015; arXiv:1508.00888 [hep-ph].

[22] U. G. Meißner and J. A. Oller, Phys. Lett. B **751**, 59 (2015), arXiv:1507.07478 [hep-ph].

[23] Michael I. Eides, Victor Yu. Petrov and Maxim V. Polyakov, Eur.Phys.J. C**78** no.1, 36 (2018).

[24] M. Karliner and J. L. Rosner, arXiv:1705.07691 [hep-ph].

[25] R. Chen, X. Liu, X. Q. Li and S. L. Zhu, Phys. Rev. Lett. **115**, no. 13, 132002 (2015), arXiv:1507.03704 [hep-ph].

[26] H. X. Chen, W. Chen, X. Liu, T. G. Steele and S. L. Zhu, Phys. Rev. Lett. **115**, no. 17, 172001 (2015), arXiv:1507.03717 [hep-ph].

[27] L. Roca, J. Nieves and E. Oset, Phys. Rev. D **92**, no. 9, 094003 (2015), arXiv:1507.04249 [hep-ph].

[28] J. He, Phys. Lett. B **753**, 547 (2016), arXiv:1507.05200 [hep-ph].

[29] L. Maiani, A. D. Polosa and V. Riquer, Phys. Lett. B **749**, 289 (2015), arXiv:1507.04980 [hep-ph].

[30] V. V. Anisovich, M. A. Matveev, J. Nyiri, A. V. Sarantsev and A. N. Semenova, arXiv:1507.07652 [hep-ph].

[31] A. Mironov and A. Morozov, JETP Lett. **102**, no. 5, 271 (2015), arXiv:1507.04694 [hep-ph].

[32] R. F. Lebed, Phys. Lett. B **749**, 454 (2015), arXiv:1507.05867 [hep-ph].

[33] V. D. Barger and R. J. N. Phillips, Phys. Lett. **B 58**, 433 (1975).

[34] S.J. Brodsky, G.F. de Teramond, I.A. Schmidt, Phys. Rev. Lett. **64** (1990) 1924.

[35] G. Gilfoyle *et al.*, https://www.jlab.org/exp_prog/proposals/07/PR12-07-104.pdf.

[36] K. A. Olive *et al.* [Particle Data Group Collaboration], "Review of Particle Physics," Chin. Phys. C **38**, 090001 (2014).